

AD-A060 666

ARMY MISSILE RESEARCH AND DEVELOPMENT COMMAND REDSTO--ETC F/G 20/6
IMAGE PROCESSING APPLICATIONS OF THE LIQUID CRYSTAL LIGHT VALVE--ETC(U)
JUN 78 J L SMITH
DRDMI-H-78-9

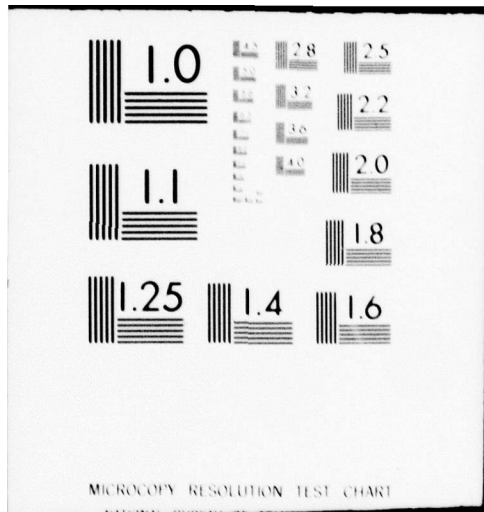
UNCLASSIFIED

NL

1 OF 1
AD
A060 666



END
DATE
FILMED
1-79
DDC



AD A060666



U.S. ARMY
MISSILE
RESEARCH
AND
DEVELOPMENT
COMMAND

DDC FILE COPY



Redstone Arsenal, Alabama 35809

DMI FORM 1000, 1 APR 77

LEVEL

9

TECHNICAL REPORT/H-78-9

DRDMI-

14 12 8.5

6

IMAGE PROCESSING APPLICATIONS OF THE
LIQUID CRYSTAL LIGHT VALVE

10

J. Lynn Smith

Technology Laboratory

DDC
NOV 1 1978
RESERVED
F

11

12 June 1978

12 29 p.

Approved for Public Release:
Distribution Unlimited.

78 10 23 6

410 127

B

DISPOSITION INSTRUCTIONS

DESTROY THIS REPORT WHEN IT IS NO LONGER NEEDED. DO NOT RETURN IT TO THE ORIGINATOR.

DISCLAIMER

THE FINDINGS IN THIS REPORT ARE NOT TO BE CONSTRUED AS AN OFFICIAL DEPARTMENT OF THE ARMY POSITION UNLESS SO DESIGNATED BY OTHER AUTHORIZED DOCUMENTS.

TRADE NAMES

USE OF TRADE NAMES OR MANUFACTURERS IN THIS REPORT DOES NOT CONSTITUTE AN OFFICIAL ENDORSEMENT OR APPROVAL OF THE USE OF SUCH COMMERCIAL HARDWARE OR SOFTWARE.



DEPARTMENT OF THE ARMY
UNITED STATES ARMY MISSILE RESEARCH AND DEVELOPMENT COMMAND
REDSTONE ARSENAL, ALABAMA 35809

DRDMI-TI

11 October 1978

SUBJECT: Errata for Technical Report H-78-9, subject: IMAGE
PROCESSING APPLICATIONS OF THE LIQUID CRYSTAL LIGHT VALVE,
by J. Lynn Smith

TO: Recipients of Subject Report

The following changes should be incorporated into subject report:

Page 21, Table 4: In "Comment" column, add "L₃ is two lens
elements with effective F.L. of 13.34 cm."

Page 23, Table 5: In lower part of table, change 1.22 mrad to
0.12 mrad and 0.17 mm to 0.017 mm.

A handwritten signature in cursive script, reading "John W. Chambers", is written over a printed name.

JOHN W. CHAMBERS
Ch, Technical Information Office
Technology Laboratory

REPORT DOCUMENTATION PAGE		READ INSTRUCTIONS BEFORE COMPLETING FORM
1. REPORT NUMBER H-78-9	2. GOVT ACCESSION NO.	3. RECIPIENT'S CATALOG NUMBER
4. TITLE (and Subtitle) IMAGE PROCESSING APPLICATIONS OF THE LIQUID CRYSTAL LIGHT VALVE		5. TYPE OF REPORT & PERIOD COVERED TECHNICAL REPORT
		6. PERFORMING ORG. REPORT NUMBER H-78-9
7. AUTHOR(s) J. Lynn Smith		8. CONTRACT OR GRANT NUMBER(s)
9. PERFORMING ORGANIZATION NAME AND ADDRESS Commander US Army Missile Research Directorate Attn: DRDMI-HR Redstone Arsenal, Alabama 35809		10. PROGRAM ELEMENT, PROJECT, TASK AREA & WORK UNIT NUMBERS
11. CONTROLLING OFFICE NAME AND ADDRESS Commander US Army Missile Research Directorate Attn: DRDMI-TI Redstone Arsenal, Alabama 35809		12. REPORT DATE 12 June 1978
		13. NUMBER OF PAGES 31
14. MONITORING AGENCY NAME & ADDRESS (if different from Controlling Office)		15. SECURITY CLASS. (of this report) UNCLASSIFIED
		15a. DECLASSIFICATION/DOWNGRADING SCHEDULE
16. DISTRIBUTION STATEMENT (of this Report) APPROVED FOR PUBLIC RELEASE. DISTRIBUTION UNLIMITED.		
17. DISTRIBUTION STATEMENT (of the abstract entered in Block 20, if different from Report)		
18. SUPPLEMENTARY NOTES		
19. KEY WORDS (Continue on reverse side if necessary and identify by block number) Liquid crystal light valve, coherent optical processing, Doppler superresolution, range slice imagery, range-Doppler image, coherent illumination, camouflage discrimination, movement detection.		
20. ABSTRACT (Continue on reverse side if necessary and identify by block number) The liquid crystal light valve (LCLV) is employed toward three distinct real-time applications in coherent optical processing. First, it is demon- strated that a real-time system for resolution improvement of distant objects (whose spin Doppler-encodes reflected laser light) is feasible. Secondly, a method for obtaining range-slice images of laboratory models is shown. Further processing, which leads to simulated range-Doppler reference images (like those obtainable from microwave radar), is then demonstrated. The third application of the LCLV uses the device integration time to discriminate		

→ next
page

UNCLASSIFIED

SECURITY CLASSIFICATION OF THIS PAGE(When Data Entered)

20. Abstract (continued)

cont. → dramatically between moving and static speckle in an input image. Real-time image discrimination of slowly moving, laser-illuminated camouflage is therefore possible. ↖

UNCLASSIFIED

SECURITY CLASSIFICATION OF THIS PAGE(When Data Entered)

LIST OF ILLUSTRATIONS

Figure		Page
1.	Structure of the Liquid Crystal Light Valve	6
2.	Optical Configuration for Doppler Superresolution Experiment	9
3.	Effect of Doppler Superresolution	12
4.	Rotating Cylinder Observation and Range-Doppler Image Representation	13
5.	Relation Between Range Slice Imagery from Cameras Observing Object along Orthogonal Axes	15
6.	Optical System Configuration for Range Slice Imagery	16
7.	Photographically Recorded Range Slice Imagery	18
8.	Time-Averaged Speckle Imaging System	20
9.	Photographic Record of Discrimination between Object in Slight Motion and Static Surroundings.....	22
10.	Oscillogram of Processed Image Intensity (Upper Trace) and Galvanometer Signal (Lower Trace)	24

LIST OF TABLES

Table	Page
1. Characteristics of the Light Valve	8
2. Experimental Parameters for Doppler Superresolution	11
3. Experimental Parameters for Range Slice Imagery	17
4. Parameters for Speckle Motion Imagery	21
5. Object Movement and Image Ratios	23

1. THE LIQUID CRYSTAL LIGHT VALVE

The function of the liquid crystal light valve (LCLV) is to transfer an input image to a spatial polarization modulation on the output. The output modulation is acquired whenever polarized readout light reflects from the output surface. An example of how an LCLV can be used is as follows:

The image of an incoherently illuminated object is focused onto the LCLV input surface. Coherent polarized laser light is collimated and, by means of a beamsplitter, directed onto and away from the output surface. An analyzer is placed in the output beam so that the spatial information becomes an intensity modulated image. Thus, the LCLV has functioned as an incoherent-to-coherent image converter. Correlation and spatial filtering processes can be applied to the image impressed on the collimated, coherent output beam. In other applications, the input may be coherent, and the output may be incoherent.

The operation of the LCLV will be briefly outlined:

An ac field of about 10 V rms is applied across the LCLV device (see *Figure 1*), in which photoconductor (CdS) and light blocking (CdTe) layers

create a rectifying heterojunction and allow some dc voltage bias to develop across the liquid crystal layer. Light incident upon the input side causes the photoconductor to become less resistive, and thus, a greater dc field appears across the liquid crystal region. The elongated nematic liquid crystals are normally parallel to the bounding insulating layers and are aligned at the boundaries according to the direction determined by ion beam etching of the layers. The crystals all try to align collectively, but a 45 degree angle twist between the etch directions at each boundary results in the twisted nematic structure developed by Schadt and Helfrich and found in *Reference 1*. Whenever the field across the liquid crystal layer is sufficiently high, the crystals tend to align with the field except near the boundaries. This breaks the collective association so that two separate, untwisted, birefringent regions exist with a difference of 45 degrees in alignment. The region first encountered by polarized readout light is oriented such that it has no effect. The second region rotates the plane of polarization of the incident and reflected light passing through it. However, when the liquid crystal field is low, the twisted molecular structure rotates and "unrotates" the incident and reflected light, having no effect on the polarization. The analyzer, through which the readout light passes, is

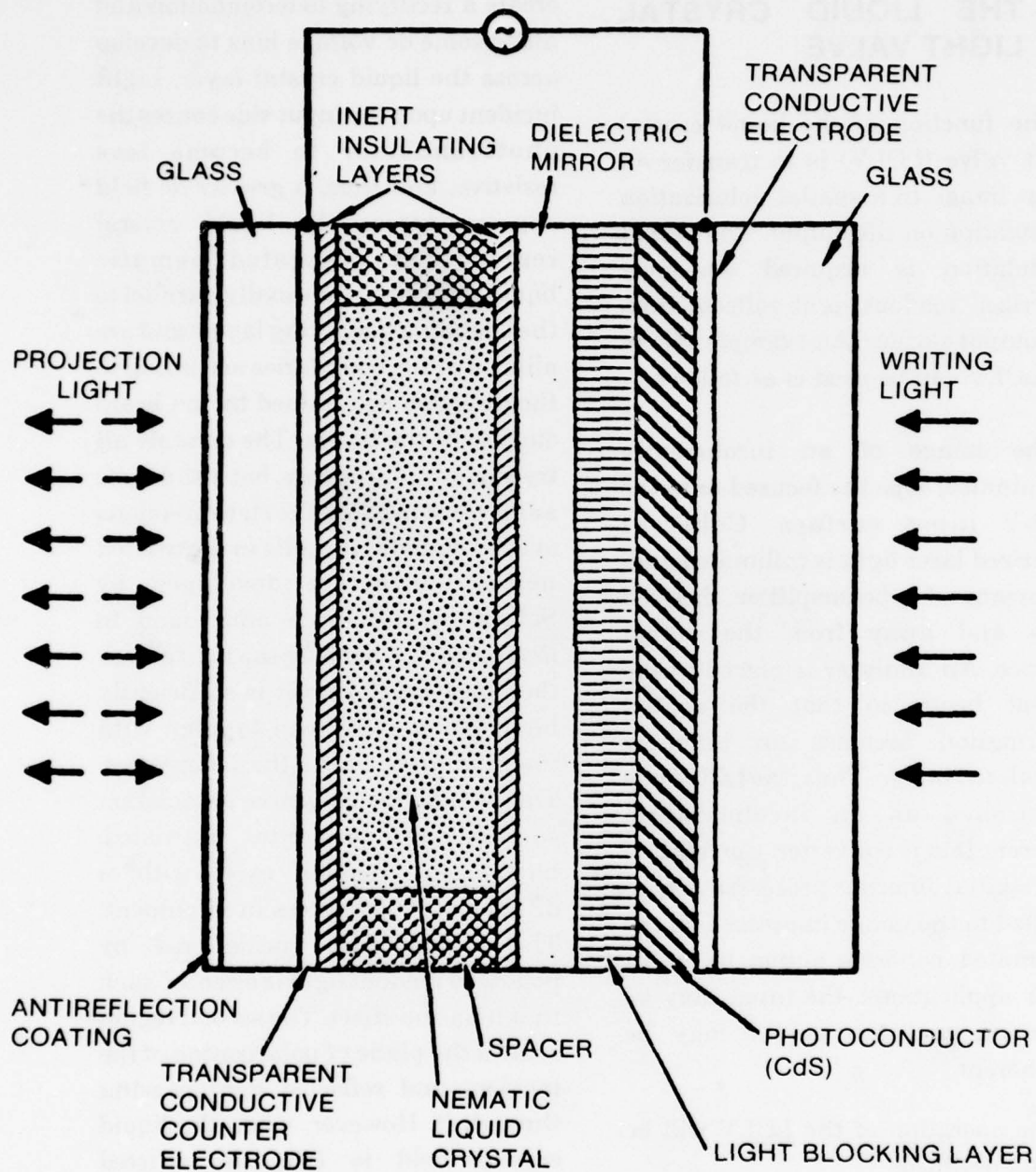


Figure 1. Structure of the Liquid Crystal Light Valve.

oriented to block the low field output (no light input) and pass the high field output (strong light input). The input and output light are separated by means of the dielectric mirror and light blocking layer shown in *Figure 1*. Further discussion on the operation of the LCLV can be found in *References 2-4*. *Table 1* lists the characteristics of the light valve as determined by the manufacturer.

In the three applications covered in this report, spatial filtering of the LCLV output is employed. By use of a beamsplitter, collimated argon-ion laser light is directed onto and away from the output surface. Two Fourier Transform lenses are positioned in the beam. The first lens is located one focal length from the LCLV and two focal lengths from the second lens. The Fourier transform plane, located midway between the lenses, contains the spatial filter, in this case an "optical dc" filter. The filter has a diameter of a few hundred microns and removes low spatial frequency content from the output image. This processing is evident in the filtered image which appears one focal length away from the second transform lens.

2. DOPPLER SUPERRESOLUTION

The principle of Doppler super-resolution is based on the fact that

the Doppler shift of coherent laser light reflected from a rotating object depends on position and angular velocity. If the plane of observation includes the axis and is normal to the line of observation, then, for given angles of incidence and reflection, the distance in this plane from the axis to the projection of a given surface element onto the plane is uniquely associated with a given Doppler shift. Hence, this "lateral" distance is Doppler encoded, and therefore, if there is lateral image degradation, the Doppler shift can be used to "reconstruct" lost information. This is accomplished by detecting immobile interference fringes between the light received from the object and a reference beam which has a lateral Doppler frequency variation.

Figure 2 depicts the optical configuration. The laser beam is split into a part for target illumination and a part for Doppler shifted reference beam formation. Doppler encoding is accomplished by rotating the reference mirror (RM) near the same velocity as the target (T). Both the target and reference mirror are imaged onto the LCLV with a slight offset angle. The lateral image quality of the target is degraded by some distorting medium (D). Near-static interference fringes only form where the target signal frequency coincides with that of the reference beam. The output side of the

TABLE 1. CHARACTERISTICS OF THE LIGHT VALVE

I. DESCRIPTION		
Liquid crystal	BDH Biphenyl Nematic	
Liquid crystal alignment	45° twisted nematic	
Aperture size	1 in. ²	
Output layer wavelength	632.8 nm	
Input image peak (photosensitivity)	525 nm (P-1 Phosphor)	
Operating voltage range	<10 V _{rms}	
Operating frequency range	1 to 100 kHz	
II. PERFORMANCE		
Operating conditions	7.9 V _{rms} at 10 kHz	
Sensitivity	Maximum transmission at 50 μW/cm ² at operating conditions	
Contrast ratio	> 100:1	
Limiting resolution	64 lines/mm at 50 μW/cm ²	
	Time response, msec	
	At 50 μW/cm ²	At 10 μW/cm ²
Rise (to 90% of maximum)	30	70
Decay (to 10% of maximum)	30	50
III. OPTICAL QUALITY		
Uniformity	Slight edge shading	
Flatness	Better than 1/4λ	
Defects	Two alignment defect areas (white light only)	
IV. CELL CONSTRUCTION		
Substrate	Sputtered DdS with SiO ₂ /TiO ₂ sputtered mirror	
Opposing electrode	1/2λ ITO with 3 layer AR on first surface— parallel to 5 sec of arc	
Cell design	Sealed	

LCLV consists of reflected laser light for which the polarization is determined by the light intensity on the input side. Hence, the output beam "picks up" the input image. The analyzer (A) and the dc spatial filter (SF) cause the final image at the screen (S) to include only correct image information. All reflected light which is non-Doppler coincident (due to distortion) is composed of fringes which move too fast to record during a sweep of the reference mirror, and hence, contribute only to near-dc spatial components which are filtered out.

The input light intensity causing fringe detection in the LCLV was approximately $1/10 \text{ mW/cm}^2$. The target image was distorted by using a lenticular screen near the back focal plane of the first detection lens. This spread the 1/2-inch image over about 2 inches. The reference and target galvanometer were sweeping 0.0375 radian in 4 seconds. Target shape was that of a flat, triangular mirror. *Table 2* lists experimental parameters used in this experiment. To reduce the effect of cosmetic defects in the LCLV, which are noticeable when the darkfield mode (optical dc filter) is employed, a negative of the defect output was made and used as a transparency filter. Photographs of the output were made with and without the optical dc filter in place so that the low resolution (or

distorted) image and the superresolved image could be compared.

Figure 3 shows the LCLV system output for the input object when undistorted, distorted, and then Doppler resolved. The distortion caused by the lenticular screen caused a lateral "smear" which was about twice the width of the LCLV window. Although the signal-to-noise in the superresolved image is not as good as one would like, the resolution improvement shown here is about a factor of 40.

Although the possibility for a real-time Doppler superresolution system has been demonstrated here, the sensitivity of the LCLV is not sufficient for direct image processing of a distant object imaged via a telephoto lens. Considerable amplification of the input image (with interference fringes due to reference beam) is necessary before the LCLV can be used. For this reason, it may be appropriate to use electronic video detection, amplification and filtering for distant, moderately illuminated objects.

3. RANGE-SLICE IMAGERY

As the name implies, range slice imagery concerns the outline of the intersection of an object with the range plane.

TABLE 2. EXPERIMENTAL PARAMETERS FOR DOPPLER SUPERRESOLUTION

PARAMETER	VALUE	COMMENT
LCLV operating voltage	25 V p - p	
LCLV operating frequency	1.5 kHz	
LCLV light input (.52 μm wavelength)	0 - 1 mW/cm ²	
Analyzer angle	73°	
First BS - T - LCLV (top path)	228 cm	same as first BS-RM-LCLV
Angles of incidence on RM, T (relative to normal)	19°, 15°	
T-LCLV path	40 cm	lens pair in this path is centered and consists of 10 in. F.L. lenses separated by 20 in.
LCLV - S path	40 cm	same applies as for the lens pair between T and LCLV
Optical dc filter diameter	200 - 400 μm	vacuum deposited Al disk
f/stop of imaging lens	5	

The range plane is located at a given range-distance from the observer and is normal to the line-of-sight. Obviously, the total area illuminated on the object between range planes (separated by some resolution distance) depends on range, object shape and object markings. Later, it will be explained exactly how the range slice imagery relates to one of its applications, range-Doppler imagery produced from microwave radar returns.

For the present, the range-Doppler observation will be discussed in its own right. *Figure 4* illustrates the

situation where an observer sees the backscatter from an illuminated, rotating cylinder. The observer could determine object reflectivity at the range plane of interest by chopping the illumination radiation into short pulses and preselecting the time interval in the backscattered pulse to make an observation. This one-dimensional return does not constitute an image because all information in the range plane is integrated. However, if the object is rotating, the Doppler shift existing normal to the rotation axis and parallel to the range plane encodes the "lateral" or x-coordinate return. Thus, except for the

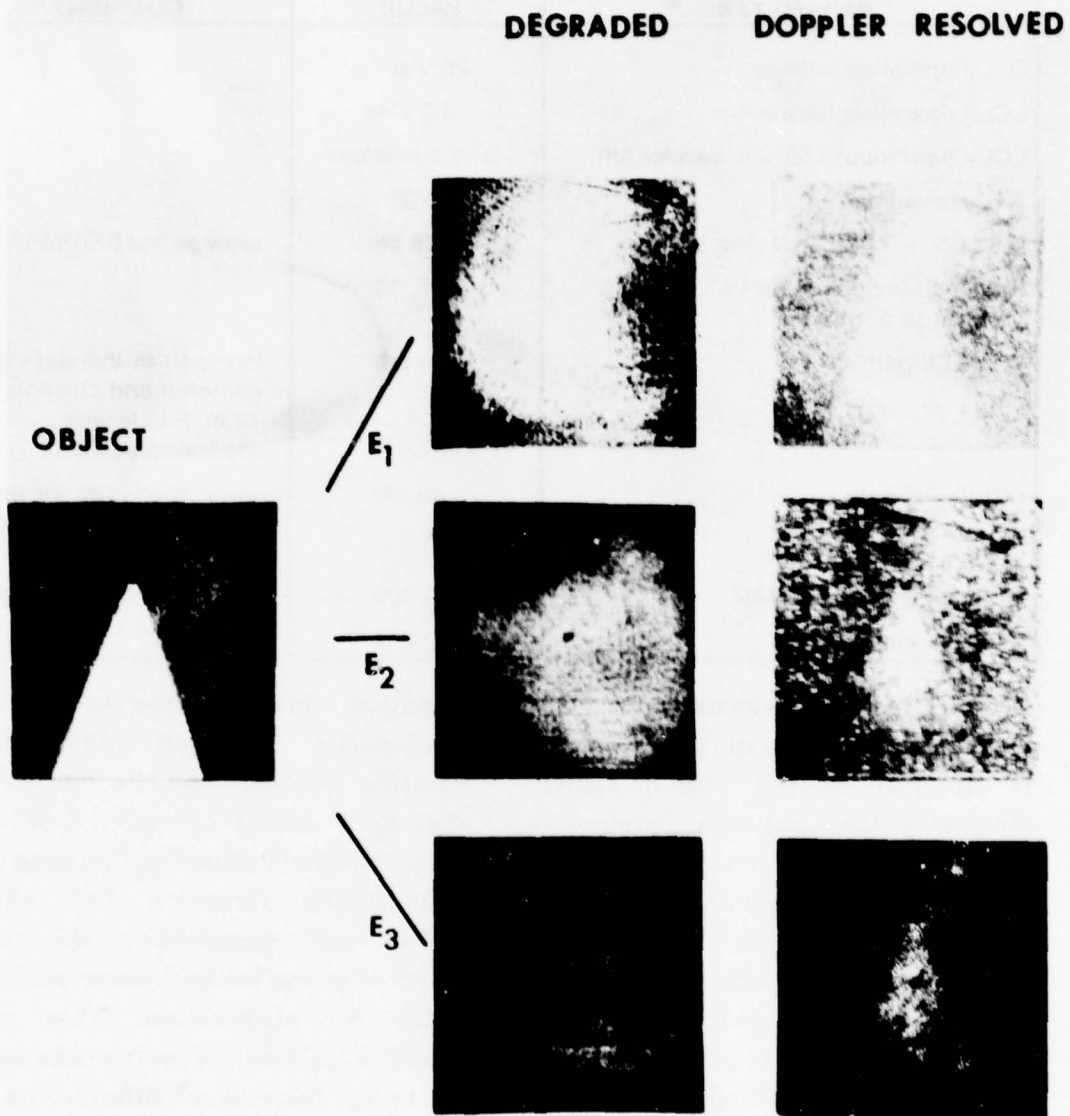
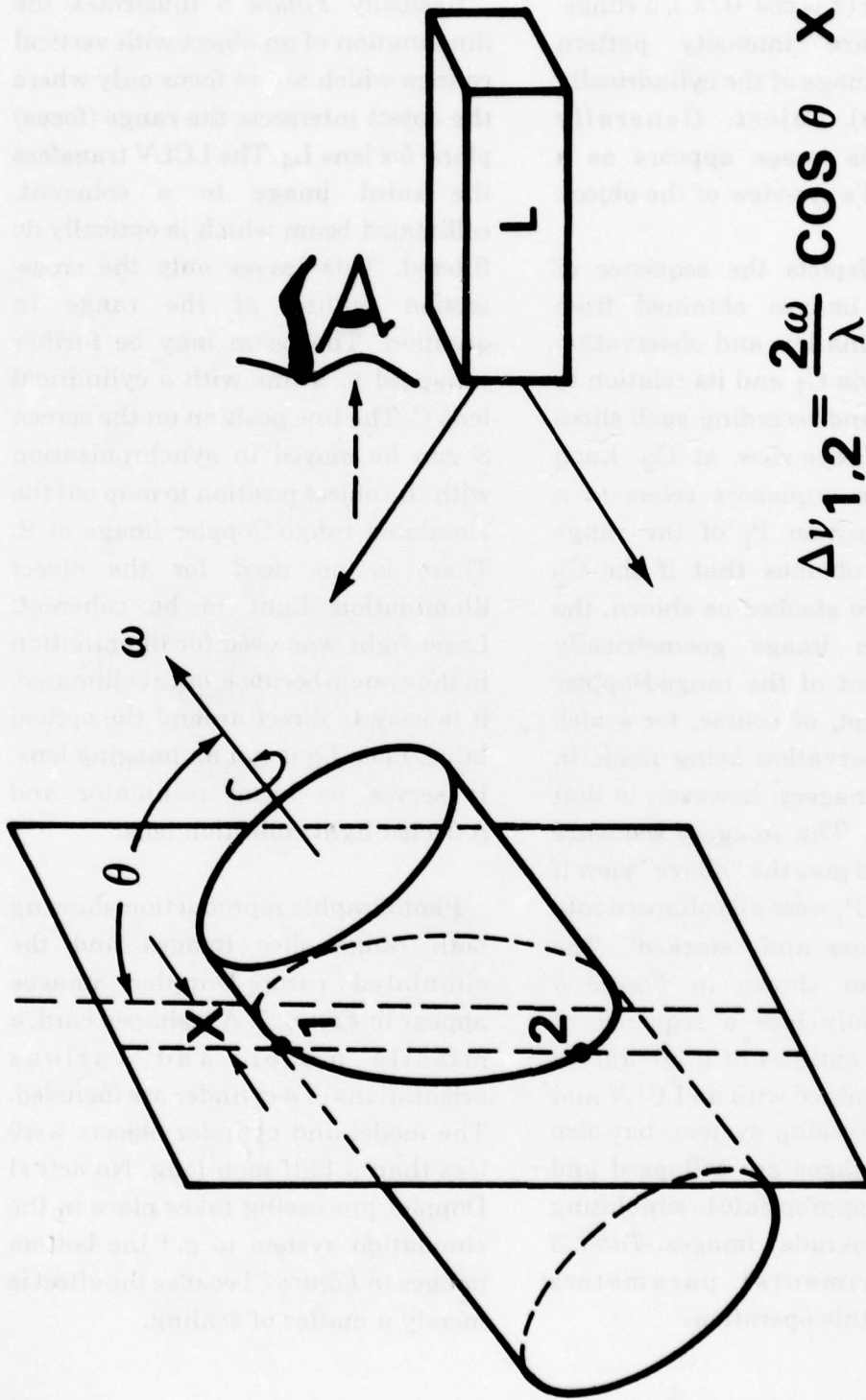


Figure 3. Effect of Doppler Superresolution. Three different exposures (E1, E2, E3) were taken photographically of the LCLV output for a flat, smooth, triangular target. The image was then degraded by lateral smearing with a lenticular screen, photographically recorded, Doppler resolved, and photographed again.



$$\Delta\nu_{1,2} = \frac{2\omega}{\lambda} \cos \theta \cdot x$$

Figure 4. Rotating Cylinder Observation and Range-Doppler Image Representation. Illumination by coherent light and backscatter detection are along the same line. The tilt of the rotation axis away from the range plane is assumed to be toward the observer. Because of rotation, the x coordinate is proportional to the Doppler shift, the scaling factor depending on rotation velocity and inclination with respect to the range plane.

scaling factor $(2 \omega \cos \theta / \lambda)$, a range-Doppler return intensity pattern presents an image of the cylindrically symmetrical object. Generally speaking, this image appears as a distorted bird's-eye-view of the object.

Figure 5 depicts the sequence of range slice images obtained from frontal illumination and observation of an object via C_1 and its relation to observation and recording such slices from a bird's-eye-view at C_2 . Each image in the sequences refers to a particular position P_i of the range plane. It is obvious that if the C_2 sequence were stacked as shown, the result is an image geometrically similar to that of the range-Doppler display (except, of course, for scale). The real observation being made in range slice imagery, however, is that made by C_1 . The imagery sequence from C_1 could give the "above" view if the circles in P_i were all collapsed into horizontal lines and "stacked". The system layout shown in *Figure 6* shows not only how a sequence of cross-section outlines of a laboratory model are obtained with an LCLV and coherent processing system, but also how these images are collapsed and stacked as is appropriate to simulating range-Doppler radar images. *Table 3* lists experimental parameters pertinent to this operation.

Basically *Figure 6* illustrates the illumination of an object with vertical rulings which are in focus only where the object intersects the range (focus) plane for lens L_4 . The LCLV transfers the ruled image to a coherent, collimated beam which is optically dc filtered. This leaves only the cross-section outline at the range in question. The beam may be further collapsed to a line with a cylindrical lens C . The line position on the screen S can be moved in synchronization with the object position to map out the simulated range-Doppler image at S . There is no need for the object illumination light to be coherent. Laser light was used for illumination in the system because, once collimated, it is easy to direct around the optical table. Lens L_3 is not an imaging lens. It serves as beam collimator and reflected light collection lens.

Photographic reproduction showing both range slice images and the simulated range-Doppler images appear in *Figure 7*. A v-shaped card, a missile model, and various orientations of a cylinder are included. The model and cylinder objects were less than a half inch long. No actual Doppler processing takes place in the simulation system to get the bottom images in *Figure 7* because the effect is merely a matter of scaling.

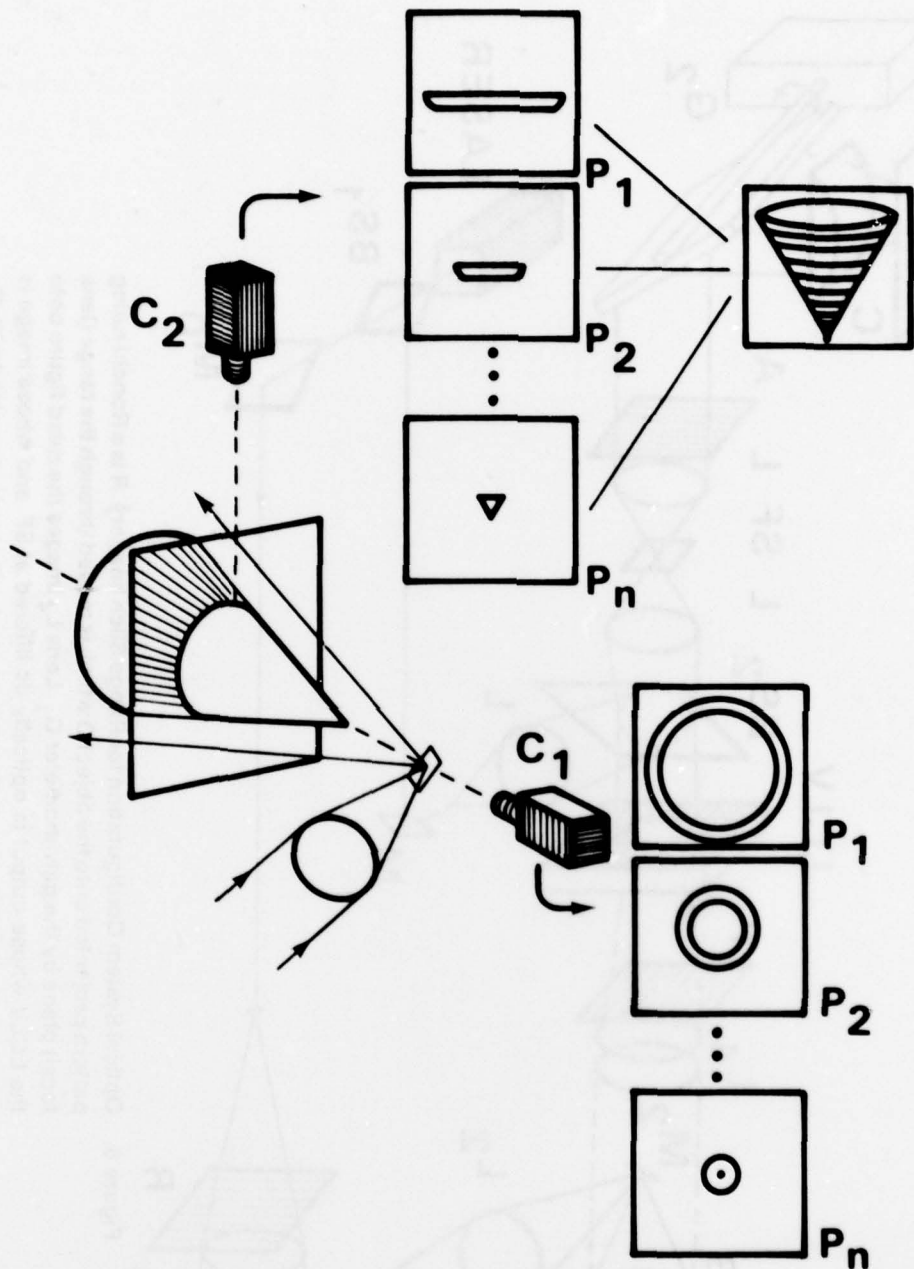


Figure 5. Relation between Range Slice Imagery from Cameras Observing Object along Orthogonal Axes. Both cameras are able to select only the illuminated outline intersecting the range plane at positions P_1, P_2, \dots, P_n . If the circular images from C_1 were "collapsed and stacked" the geometrical result would be the same as that from C_2 .

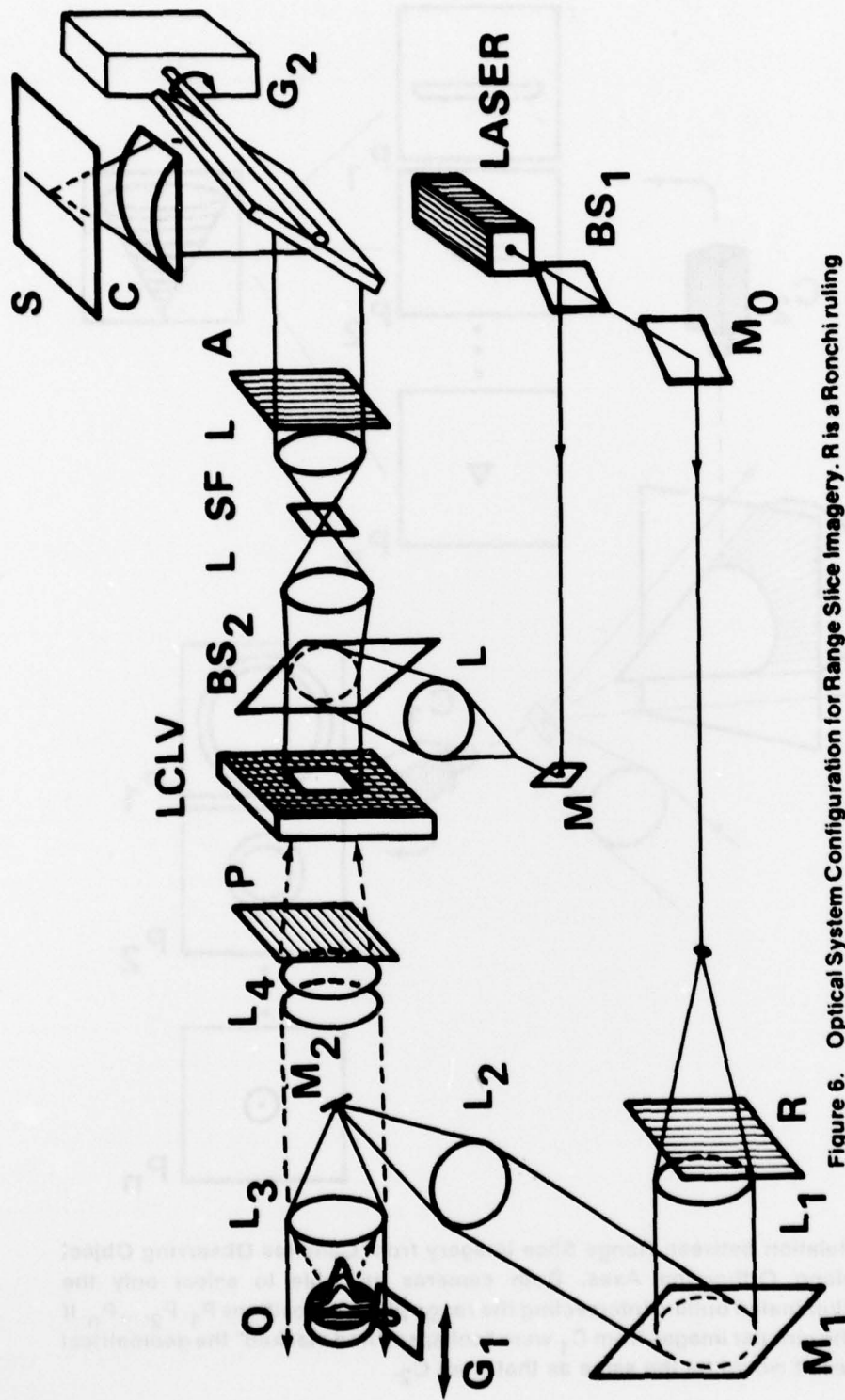


Figure 6. Optical System Configuration for Range Slice Imagery. R is a Ronchi ruling pattern projected onto the object O which is moved through the range (lens focal) plane by the galvanometer G_1 . Lens L_4 images the ruled figure onto the LCLV whose output is optically dc filtered at SF, and whose image is collapsed by C to a line on S. The galvanometer G_2 is synchronized with G_1 so that the line sweeping across S defines the figure in terms of horizontal and range coordinates.

TABLE 3. EXPERIMENTAL PARAMETERS FOR RANGE SLICE IMAGERY

PARAMETER	VALUE	COMMENT
LCLV operating voltage	30-35 V p-p	
LCLV operating frequency	1.5 kHz	
LCLV light input (.52 μm wavelength)	0 to 1 mW/cm ²	
Analyzer angle	90°	
Ruling (R) — L ₁ distance	5.1 cm	center-to-center (c-c)
L ₁ — L ₃ path	53 cm	L ₃ is a Cannon® 50 mm f/stop 1.8 camera lens
L ₃ — L ₄	27 cm	(c-c)
LCLV — L	26 cm	(c-c)
L — SF — L	51 cm	each L is a 10 inch F.L. lens
L — C	27 cm.	C is at point of best focus
L — S	36 cm	
Optical dc filter diameter	200 - 400 μm	vacuum deposited Al disk
f/stop of input imaging lens (L ₄)	2.5	light collection determined by L ₃ (used as magnifier) as well as L ₄
Ronchi Ruling Spacing	50 lines/inch	

Applicability of the range slice imagery system to range-Doppler radar consists in compiling a catalog of images for various object shapes, angular velocities and angles of inclination. Such a reference catalog would not necessarily be in the form of a book; it may be stored somewhere in a system for purposes of image correlation and identification.

4. TIME-AVERAGED SPECKLE IMAGERY

When objects are camouflaged to blend with surroundings, detection is

usually difficult unless there is significant object movement. One way to enhance the effect of slight movement is to illuminate the scene with laser light, project it onto a screen with an imaging lens, and observe the speckled image. Because object movements may be very small and still cover many wavelengths, the speckle comprising the image regions in slight motion will dart about and scintillate rapidly. However, the speckle in immobile regions remains fixed. If a time exposure were made, during which the object moved slightly, the

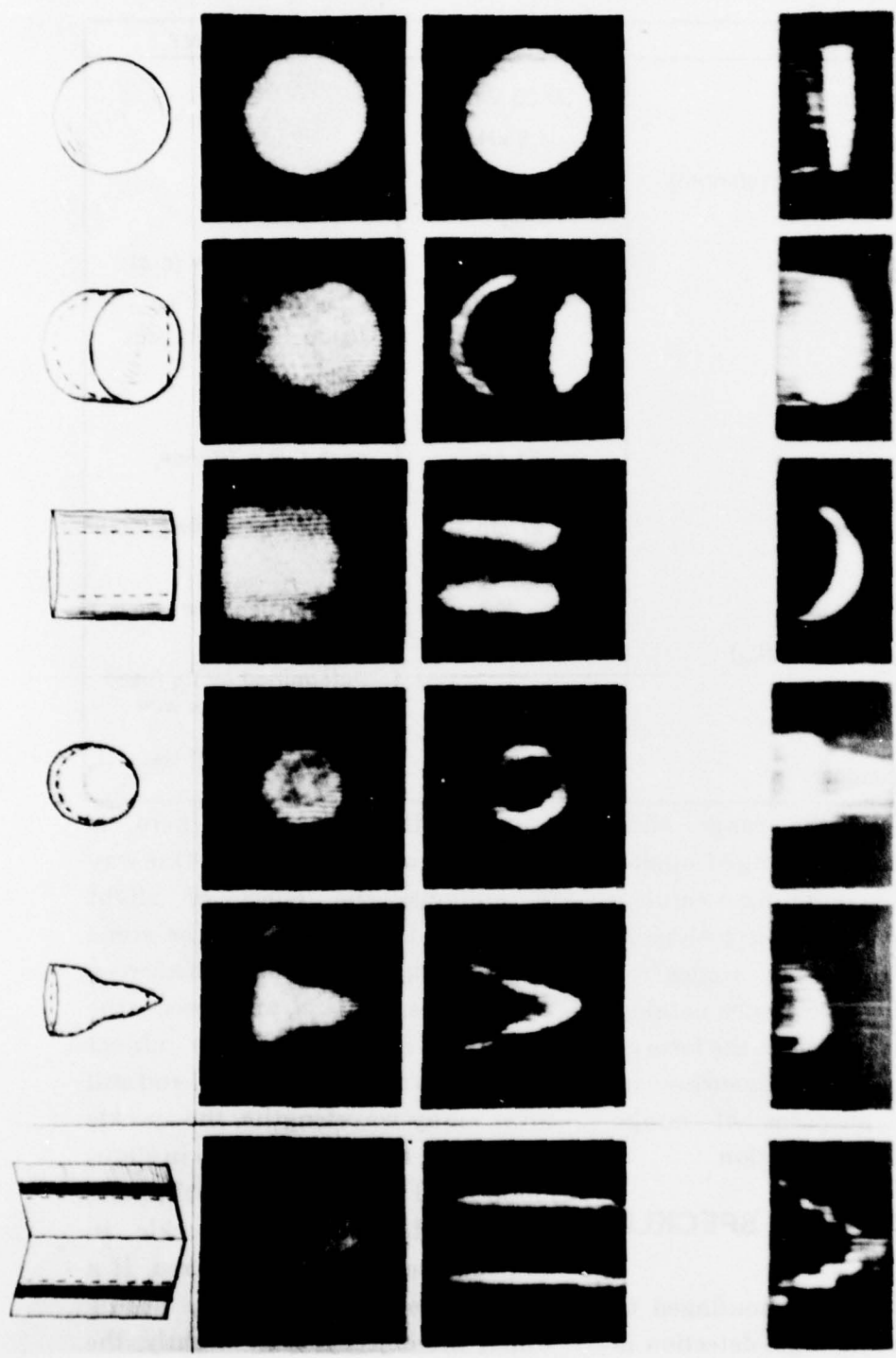


Figure 7. Photographically Recorded Range Slice Imagery. Each column represents a progression through the system. At the top is a sketch of the object, showing its orientation in the range (focus) plane; second down, is the unfiltered output image of the LCLV, third, is the dc filtered output which shows the illuminated outline of a slice; at the bottom, is the combined exposure of all such slices collapsed to a horizontal line which sweeps vertically as the object moves through the range (focal) plane. The bottom image appears to be a "bird's-eye-view", although image detection was from the front.

image would have the low spatial frequency content of time-averaged speckle in moving regions and high spatial frequency content in the static regions.

The LCLV has a rise and fall response time during which any image projected onto it is integrated into one "exposure" segment of real-time operation. It is this integration time (30-100 msec) along with coherent illumination and finite imaging lens aperture that makes the LCLV suitable as a slight-motion discriminator. The output of the LCLV is optically dc filtered to attenuate low frequency content in the resultant image. Thus, the moving regions appear silhouetted against static surroundings.

Figure 8 shows the optical setup in the time-averaged speckle imagery demonstration, and *Table 4* lists the experimental parameters selected. The object was an upright arrow (connected to an oscillating galvanometer) which was covered with non-smooth foil surface and markings similar to that of its immediate environment. Object velocities from 1 mm/sec to 60 mm/sec were noted, the most silhouetting associated with the highest motion.

Figure 9 shows photographic proof of the discriminating ability in time-

averaged speckle imagery. In these demonstrations, the object was oscillating at 15 Hz with an amplitude of about .5 mm.

After the imagery demonstration, the silhouetting effect was studied quantitatively.

A column of *Table 5* displays the object motion in terms of the angular velocities it makes with respect to the imaging lens as it traverses a portion of the field of view. The next column contains the corresponding ratios of the object's processed image intensity when in motion to that when static. The *f*/stop number and diffraction-limited resolution are also included.

Figure 10 is an oscillogram of the object's processed image intensity detected by a photodiode (upper trace) and also the object's galvanometer signal (lower trace). The object motion is linear in time. The rise and decay times seen are properties of the LCLV in this application.

In real situations, an object's movements would be discontinuous, and the silhouetting effect would come and go, further accenting the region where movement takes place. If the object is to be illuminated weakly with laser light, and/or if the observer must use a small telephoto-type lens, light intensification is necessary. Two or

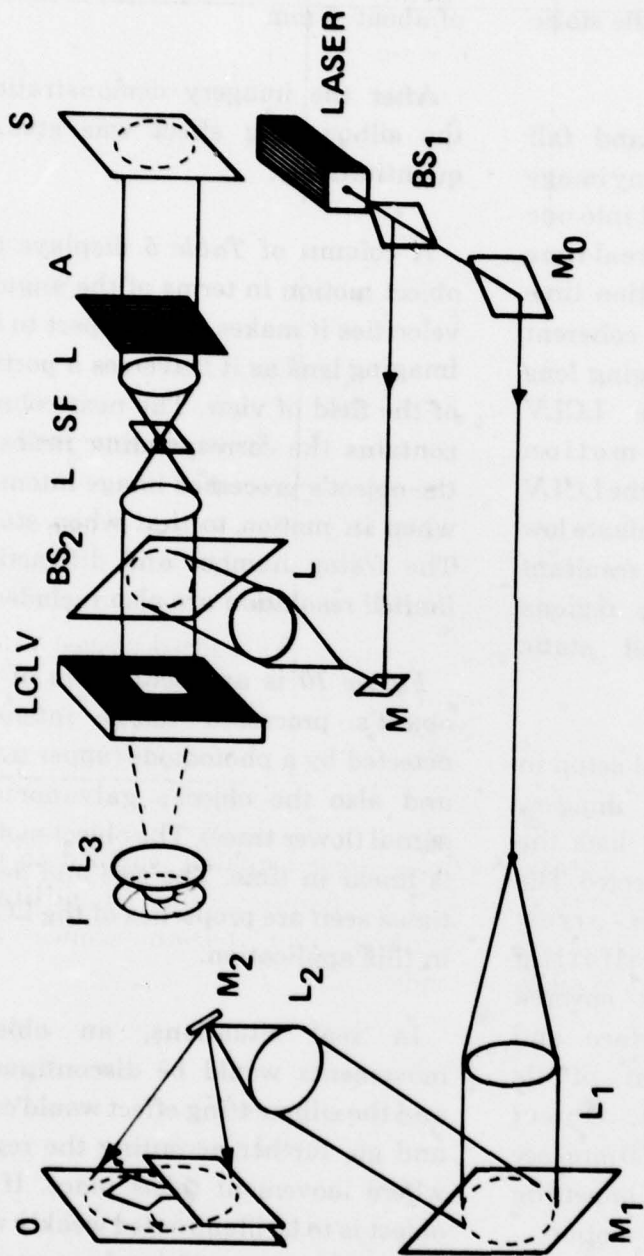


Figure 8. Time-Averaged Speckle Imaging System. A vertical arrowhead-shaped object O oscillates slightly in a foreground and background of similar reflectivity and markings. Laser illumination of O and the finite aperture permitted by the iris I cause L₃ to project a speckled image onto the LCLV. The output of LCLV is optically dc filtered at SF and imaged at S.

TABLE 4. PARAMETERS FOR SPECKLE MOTION IMAGERY

PARAMETER	VALUE	COMMENT
LCLV operating voltage	30 V p-p	
LCLV operating frequency	1.5 kHz	
LCLV light input (.52 μm wavelength)	0 to 1 mW/cm ²	
Analyzer angle	80°	
M ₂ - 0 distance	35.5 cm	
"Arrow" target size	2 cm × 2.5 cm	
O - I distance	50.8 cm	
I opening diameter	.635 cm	
I - L ₃	2.5 cm	
L ₃ - LCLV	17.8 cm	center-to-center (c-c)
LCLV-L	26 cm	(c-c)
L-SF-L	51 cm	each L is a 10 inch F.L. lens
L - S	26 cm	
Optical dc filter diameter	400 - 600 μm	vacuum deposited Al disk
Object movement	.5mm at 15 Hz - 2mm at 1 Hz	
f/stop of input imaging lens (with iris)	21	

three state-of-the-art solid state intensifier layers might give 400-1000 increase in intensity. The resolution must be sufficient so that the speckle

fields are adequately coupled to the LCLV. Applications in military sighting and reconnaissance are evident.

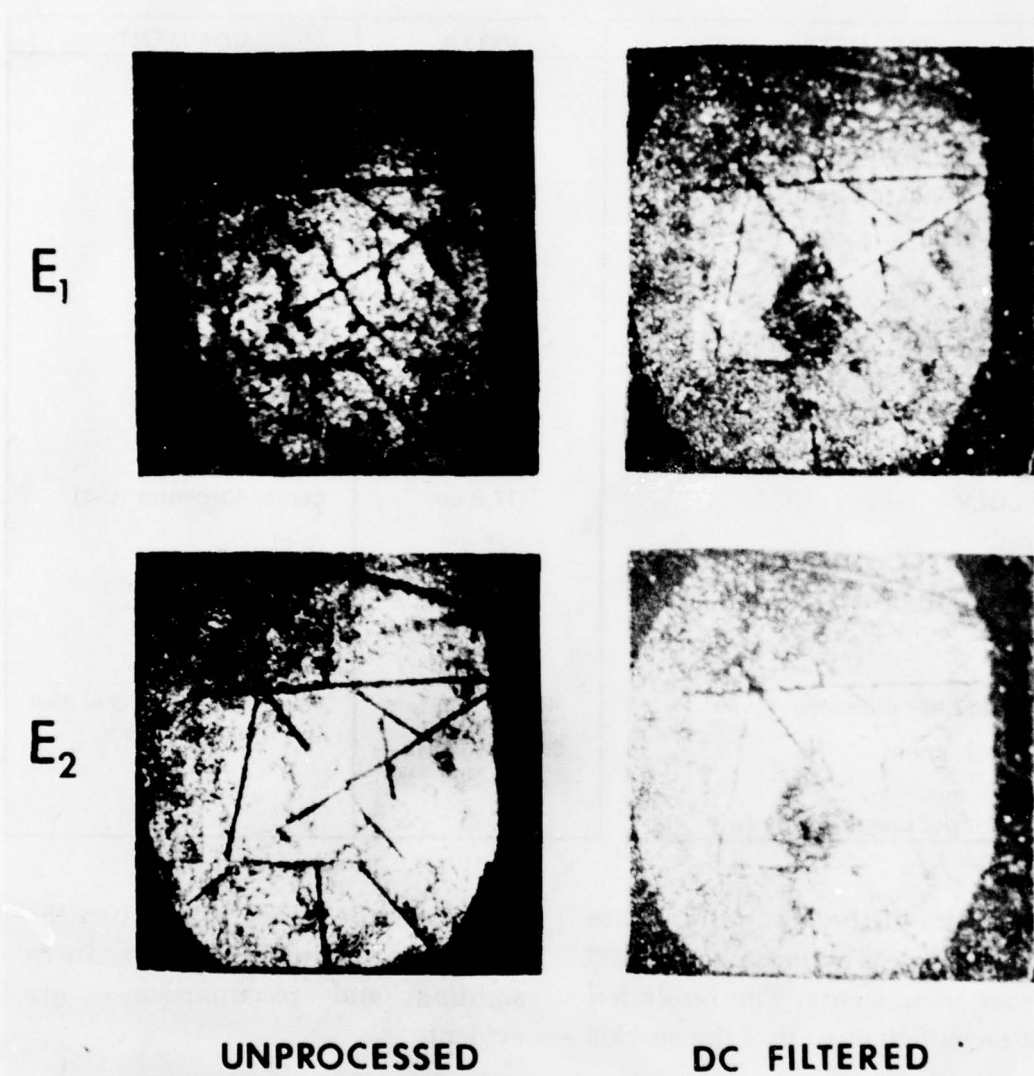


Figure 9. Photographic Record of Discrimination between Object in Slight Motion and Static Surroundings. Two exposures E_1 and E_2 show (l) the unprocessed image output of the LCLV for the laser illuminated object and (r) the optically dc filtered output which reveals the arrowhead-shaped object.

TABLE 5. OBJECT MOVEMENT AND IMAGE RATIOS

OSCILLOGRAM NO.	LENS-OBJECT ANGULAR VELOCITY (deg/sec)	I_R/I_P *
---	.000	1.00
5c	.012	.70
4c	.025	.59
1c	.153	.35
3c	.385	.19
2c	1.533	.06

Resolution ** of imaging lens --- 1.22 mrad (.17mm at LCLV)
f/stop of imaging lens --- 27

* I_R is the image intensity when object moves and I_P is that when the object is immobile

** Diffraction limited and focus for infinity

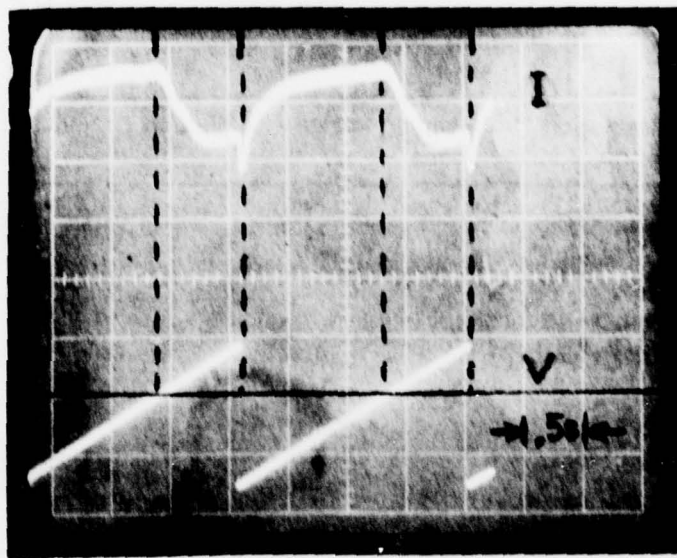


Figure 10. Oscillogram of Processed Image Intensity (upper trace) and Galvanometer Signal (lower trace). The object moves linearly when the driving signal rises above the dark horizontal line. During motion, the intensity drops to a constant value and then dips further as the object snaps back to its original position at the end of the signal ramp. When the signal voltage is below the black horizontal line, the object is motionless and the intensity rises back toward a peak value.

REFERENCES

1. M. Schadt and W. Helfrich, *Appl. Phys. Lett.* 18, 127 (1971).
2. J. Grinberg, et al., *Optical Engineering* 14, 217 (1975).
3. A. D. Jacobson, et al., *Annals of the New York Academy of Science* 267, 417 (1976).
4. J. Grinberg, et al., *Effective Utilization of Optics in Radar Systems, SPIE* 128, 253 (1977).

DISTRIBUTION

	No. of Copies		
Defense Documentation Center Cameron Station Alexandria, Virginia 22314	12	Commander US Army Electronics R&D Command ATTN: DRSEL-TL-T, Dr. Jacobs DRSEL-CT, Dr. R. Buser Fort Monmouth, New Jersey 07703	1 1
Commander US Army Research Office ATTN: Dr. R. Lontz P O Box 12211 Research Triangle Park, North Carolina 27709	2	Director US Army Night Vision Laboratory ATTN: John Johnson Fort Belvoir, Virginia 22060	1
US Army Research and Standardization Group (Europe) ATTN: DRXSN-E-RX, Dr. A. Nedoluha Box 65 FPO, New York 09510	2	Commander US Army Picatinny Arsenal Dover, New Jersey 07801	1
Commander US Army Materiel Development and Readiness Command ATTN: DRCLDC, Dr. G. Bushy DRCLDC, Mr. J. Bender DRCDE-D, Mr. E. Sedlak 5001 Eisenhower Avenue Alexandria, Virginia 22333	1 1 1	Commander US Army Foreign Science and Technology Center ATTN: W. Alcott Federal Office Building 220 Seventh Street NE Charlottesville, Virginia 22901	1
HQ, Department of the Army DAMA-ARZ Washington, D. C. 20310	2	Commander US Army Training and Doctrine Command Fort Monroe, Virginia 22351	1
Director of Defense Research and Engineering Engineering Technology ATTN: Mr. L. Weisberg Washington, D. C. 20301	2	Director Ballistic Missile Defense Advanced Technology Center ATTN: ATC-D ATC-O ATC-R ATC-T P. O. Box 1500 Huntsville, Alabama 35808	1 1 1 1
Director Defense Advanced Research Projects Agency ATTN: MAJ Karem Mr. D. Walsh 1400 Wilson Boulevard Arlington, Virginia 22209	1 1	Commander US Naval Air Systems Command Missile Guidance and Control Branch Washington, D. C. 20360	1
Commander US Army Aviation Systems Command 12th and Spruce Streets St. Louis, Missouri 63166	1	Chief of Naval Research Department of the Navy Washington, D. C. 20360	1
Director US Army Air Mobility Research and Development Laboratory Ames Research Center Moffett Field, California 94035	1	Commander US Naval Air Development Center Warminster, Pennsylvania 18974	1
		Commander US Naval Electronics Lab Center San Diego, California 92152	1

Director		Commander (AFEL)	1
Naval Research Laboratory		Hanscom Air Force Base, Maryland 01731	
ATTN: Code 5570, D. Ringwolt	1		
Code 5570, T. Giallorinzi	1	Commander	1
Washington, D. C. 20390		AFATL/LMT, C Warren	
		Eglin Air Force Base, Florida 32544	
Commander			
Center for Naval Analyses		Environmental Research Institute of Michigan	
ATTN: Document Control	1	Radar and Optics Division	
1401 Wilson Boulevard		ATTN: Dr. A. Kozma	1
Arlington, Virginia 22209		Dr. C. Aleksoff	1
		P. O. Box 618	
McDonnell Douglas Research Institute		Ann Arbor, Michigan 41807	
ATTN: Dr. C. Leader	1		
Box 516		National Bureau of Standards	
St Louis, Missouri 63166		ATTN: E. Johnson, Jr.	1
		325 South Broadway	
Brown Engineering Company		Boulder, Colorado 80302	
ATTN: Dr. Harry Watson	1		
300 Sparkman Drive		Naval Avionics Facility	1
Huntsville, Alabama 35807		Indianapolis, Indiana 46218	
Optical Science Corporation		Science and Technology Division	
ATTN: Dr. David Fried	1	Institute of Defense Analysis	
P. O. Box 388		ATTN: Dr. V. Corcoran	1
Yorba Linda, California 92686		Dr. M. Hammond	1
		400 Army-Navy Drive	
Department of Electrical Engineering		Arlington, Virginia 22202	
Stanford University			
ATTN: Dr. J. W. Goodman	1	DRCPM-PE	1
Palo Alto, California 94305		DRSMI-LP, Mr. Voigt	1
		DRDMI-XS, Dr. Hallows	1
Optical Sciences Center		DRDMI-NS, Mr. Hagood	2
University of Arizona		DRDMI-C	1
ATTN: Dr. W. L. Wolfe	1	DRDMI-Y	1
Tucson, Arizona 85721		DRDMI-HR, Dr. Hartman	1
		Dr. Bennett	1
University of Rochester		DRDMI-HRO, Dr. Christensen	1
College of Engineering and Applied Science		Dr. Guenther	1
Institute of Optics		Dr. Smith	20
ATTN: Dr. N. George	1	Dr. Stettler	1
Rochester, New York 14627		DRDMI-T, Dr. Kobler	1
		Mr. Fagan	1
Commander		DRDMI-TD	1
Rome Air Development Center		DRDMI-TE, Mr. Pittman	1
US Air Force		Mr. Russell	1
ATTN: J. Wasielewski, IRRC	1	Dr. Kulas	1
Griffis Air Force Base, New York 13440		DRDMI-TG	1
		DRDMI-TBD	3
Commander		DRDMI-TI (Record Set)	1
US Air Force, AFOSR/NE		(Reference Set)	1
ATTN: Dr. J. Neff, Building 410	1		
Bolling Air Force Base		IIT Research Institute	1
Washington, D. C. 20332		ATTN: GACIAC	
		10 West 35th Street	
Commander		Chicago, Illinois 60616	
US Air Force Avionics Laboratory			
ATTN: W. Schoonover	1		
Dr. E. Champaign	1		
Dr. J. Ryles	1		
G. Urban	1		
Wright-Patterson Air Force Base, Ohio 45433			